

Soft Matter

Accepted Manuscript



This is an *Accepted Manuscript*, which has been through the Royal Society of Chemistry peer review process and has been accepted for publication.

Accepted Manuscripts are published online shortly after acceptance, before technical editing, formatting and proof reading. Using this free service, authors can make their results available to the community, in citable form, before we publish the edited article. We will replace this *Accepted Manuscript* with the edited and formatted *Advance Article* as soon as it is available.

You can find more information about *Accepted Manuscripts* in the [Information for Authors](#).

Please note that technical editing may introduce minor changes to the text and/or graphics, which may alter content. The journal's standard [Terms & Conditions](#) and the [Ethical guidelines](#) still apply. In no event shall the Royal Society of Chemistry be held responsible for any errors or omissions in this *Accepted Manuscript* or any consequences arising from the use of any information it contains.

On the mechanisms of colloidal self-assembly during spin-coating.

Daniel T. W. Toolan, Syuji Fujii, Stephen J. Ebbens, Yoshinobu Nakamura and Jonathan R. Howse*

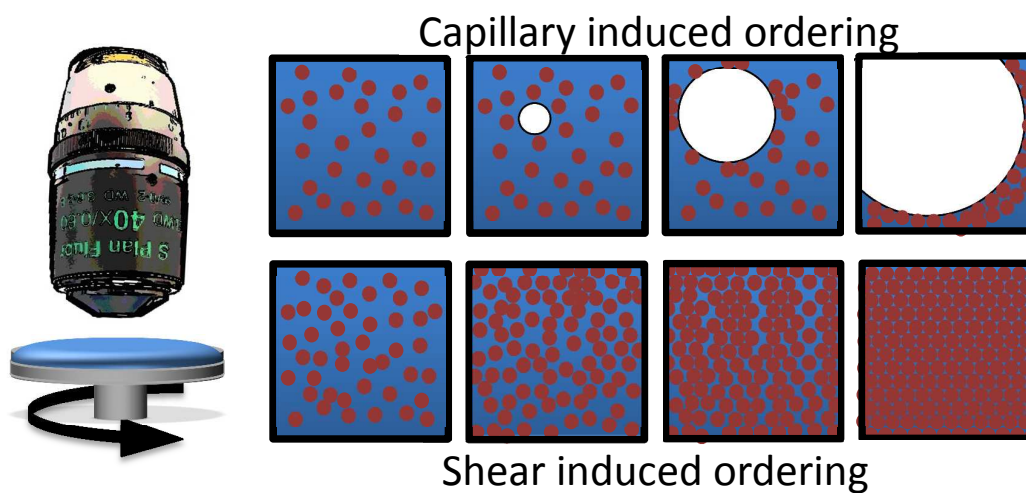
Dr. D. T. W. Toolan, Dr. S. Ebbens, Dr. J. R. Howse

Department of Chemical and Biological Engineering, The University of Sheffield, Sheffield S1 3JD, UK.

E-mail: j.r.howse@sheffield.ac.uk

Dr. S. Fujii, Prof. Y. Nakamura

Department of Applied Chemistry, Faculty of Engineering, Osaka Institute of Technology 5-16-1 Ohmiya, Asahi-ku, Osaka 535-8585, Japan

TOC

Through the technique of stroboscopic microscopy we are able to directly identify a number of different mechanisms by which colloids self-assemble during spin-coating.

Abstract

Spin-coating offers a facile fabrication route for the production of high quality colloidal crystals, which have potential as photonic band-gap materials. This paper presents the results of direct observations of the self-assembly of latex colloids during spin-coating through the use of stroboscopic microscopy. We have been able to identify several mechanisms by which self-assembly occurs, depending upon the dispersion properties, such as particle weight fraction, solvent volatility and viscosity. Through the use of stroboscopic microscopy we have directly observed ordering occurring due to high concentrations of colloid particles (where volatility is relatively low), resulting in the formation of regular close packed ordered particle arrays. Conversely when the system is spun-cast from a much more volatile solvent, highly disordered non-equilibrium arrangements of particles form. When spin-coating a low concentration, low volatility dispersion, ordering is dominated by the occurrence of capillary drying fronts, which drag the particles into ordered arrangements. At a certain volatility, intermediate to that of water and ethanol, ordering occurs predominantly via shear forces. Finally when the volatility is increased beyond the shear ordering regime, excessive shear leads to the occurrence of drying fronts within the system and so again, capillary force induces a large degree of order within the final film.

The self-organisation of colloidal dispersions is a highly important and promising phenomenon, which has been a topic of intense scientific interest due to the applications of latex films in a wide range of applications including coatings, adhesives and inks.¹⁻³ A crucial stage in latex film formation is the evaporation of solvent from a colloidal dispersion, resulting in particle ordering and packing into three dimensional structures. Beyond latex film formation the self-organisation of colloids influences processes as varied as the formation of dense ring-like deposits when coffee is spilled on a surface⁴ and the formation of highly ordered two and three dimensional crystalline structures known as colloidal crystals, which have potential applications as photonic band-gap materials.⁵ One of the main obstacles to exploiting these exciting materials is developing and understanding fabrication strategies that allow for fine control over the complex self-assembly processes that occur, such that large, defect free colloidal crystals may be obtained, via industrially scalable manufacturing methods.

Colloidal dispersions possess a rich variety of phase behavior, mimicking that of simple atomic liquids and solids, such that as the particle concentration is increased a transition from a disordered arrangement of particles to a highly ordered arrangement of particles may be observed, analogous to liquid and crystalline phases,⁶ where the transitions may be described by an effective hard-sphere model.⁷

Well ordered two and three dimensional particle arrays often spontaneously form when a colloidal dispersion is deposited on a solid substrate, where the self-assembly of particles may occur via convective assembly. This process involves the formation of a crystal nucleus (comprising of a small number of colloids) through attractive capillary forces, and subsequent crystal growth driven by convective

particle flux caused by water evaporation from the ordered crystalline regions.⁸ Additionally, colloids can form well ordered two and three dimensional ring structures which may form via two different mechanisms. The most familiar instance being the “coffee ring effect”, where some particles irreversibly stick to the substrate at the drop periphery under the action of capillary forces, pinning the contact line, resulting in evaporation from the edge being compensated by flow from the interior. This pulls suspended particles to the drop periphery, producing a ring of particles.⁹ Alternatively, in some cases surface forces may induce film destabilisation and hole formation. The rim of the expanding capillary front of the wetting film drags the particles away, arranging them into annular rings.¹⁰

Spin-coating is a thin film production technique widely utilised for semiconductor fabrication that has since been demonstrated as a facile method for the production of highly uniform colloidal crystal thin films.¹¹⁻¹⁶ Such films may be either mono or multi layered and are often polycrystalline with a high degree of long range orientation about the spinning axis.¹⁷ The technique involves depositing a colloidal dispersion onto an optically flat substrate that is then rotated at high-speed (1,000 – 10,000 RPM). Fluid thinning occurs due to both shear forces and evaporation of the dispersant, resulting in the formation of a dry film within a matter of seconds.^{18,19} However, the rapidly rotating sample and high evaporation rates make performing studies *in situ* challenging and as such the majority of studies have been performed *ex situ*, where the final ordered structure is analysed and used to produce an inferred hypothesis based upon theory and macroscopic observations. Such approaches are far from ideal, especially as complex coating procedures are

often employed, comprising of a number of different rotation rates, acceleration rates and hold times.¹⁵

Guiliani *et al* utilised high speed imaging to study symmetry transitions that occur during the spin-coating of silica particles (~460 nm) from methyl ethyl ketone (MEK) and acetone, where transitions from six-fold to four-fold and back to six-fold symmetries were observed, corresponding to either hexagonal (six-fold) or square (four-fold) arrangements of particles in the substrate plane.²⁰ Such symmetries occur due to long range translational ordering of the particles. Due to the geometry of this experimental set-up any symmetry observed is two dimensional, parallel to the plane of the substrate. A drawback of this approach is that as these symmetries arise as a consequence of ordering and it is therefore not possible to directly ascertain the absolute mechanism through which ordering proceeded as observations are made in a scattering geometry and thus are based in reciprocal space.

There are numerous factors that affect structure formation of spin-coated colloidal crystals which may be described as dispersion properties and spin-coating parameters. Dispersion properties include particle size, size distribution, dispersant (volatility, viscosity), dispersant mixture (often dispersant mixtures are employed to tune properties such as solvent evaporation rate profiles) and the particle concentration.¹¹⁻¹³ Spin-coating parameters include the rotation and acceleration rates, which influence how the colloidal mixture is spread and subsequently dries.^{15,21}

Until recently it has not been possible to directly observe (in real-space) the finer details of self-assembly processes during spin-coating. The “optostrobometer”,²²⁻²⁵ is a stroboscopic microscopy technique that has recently

been utilised to directly observe the processes of phase separation and crystallisation in spin-coated polymer blends. In the study we present here, we have employed this technique to directly observe colloidal crystallisation during spin-coating which yield highly ordered crystalline structures. Importantly we are able to observe a variety of different mechanisms by which ordering proceeds and to what extent these different processes control both intermediate and final morphologies of colloidal crystals.

In this particular study we have looked at relatively large (by colloidal crystal standards) colloids in water, ethanol, and mixtures of the two solvents, at a variety of weight percents and solvent mixture ratios. Figures 1 – 3 show a series of stroboscopic microscopy images obtained at the center of the rotating sample (along with corresponding reciprocal space Fast Fourier transforms to help quantify the order within the system) taken during spin-coating of colloidal dispersions of 5 μm polystyrene particles in water at 1250 rpm, at concentrations of 25, 35 and 45 wt%, respectively.

The stroboscopic data for the 25 wt% dispersion (**Fig 1. and Supporting information - MOVIE #1**) show that initially, the dispersion and particles flow towards the bottom left of the image until ~ 4.8 s. During this initial flow stage the particles move in clusters. The reciprocal space FFT images reveal a diffuse ring,^a indicating that the particles within these clusters are arranged loosely and randomly and do not possess the high degree of order, characteristic of crystalline ordering. We ascribe this initial radial flow of the particles to shear thinning of both components of the colloidal dispersion. Between $\sim 5 - 8$ s, the particles then move towards the top of the image, this change in the direction of particle flow arises from a transition

from shear thinning to evaporative thinning. Shear forces act as a result of the rotation of the sample and thus the direction of such forces is fixed, and away from the center of rotation. The change in the direction of the forces acting upon the colloidal dispersion gives further evidence to the change in the origin of the forces dominating colloid flow and consequent ordering. At 10.1 s, the particles begin to order due to capillary effects, where an ordered monolayer of regularly close packed particles forms due to the random appearance of holes in the wetting film, which subsequently force the particles to be displaced along the drying fronts as the wetting film recedes. The observation of the growth of drying fronts as the film evaporates is consistent with observations of Elbaum and Lipson, who studied the evaporation of water on freshly cleaved mica.²⁶

The morphology becomes fixed at ~16s, comprising of highly crystalline regions containing large open voids. The FFT of the final structure shows a large number of bright spots at uniform distance from the center and indicative of a final polycrystalline film.

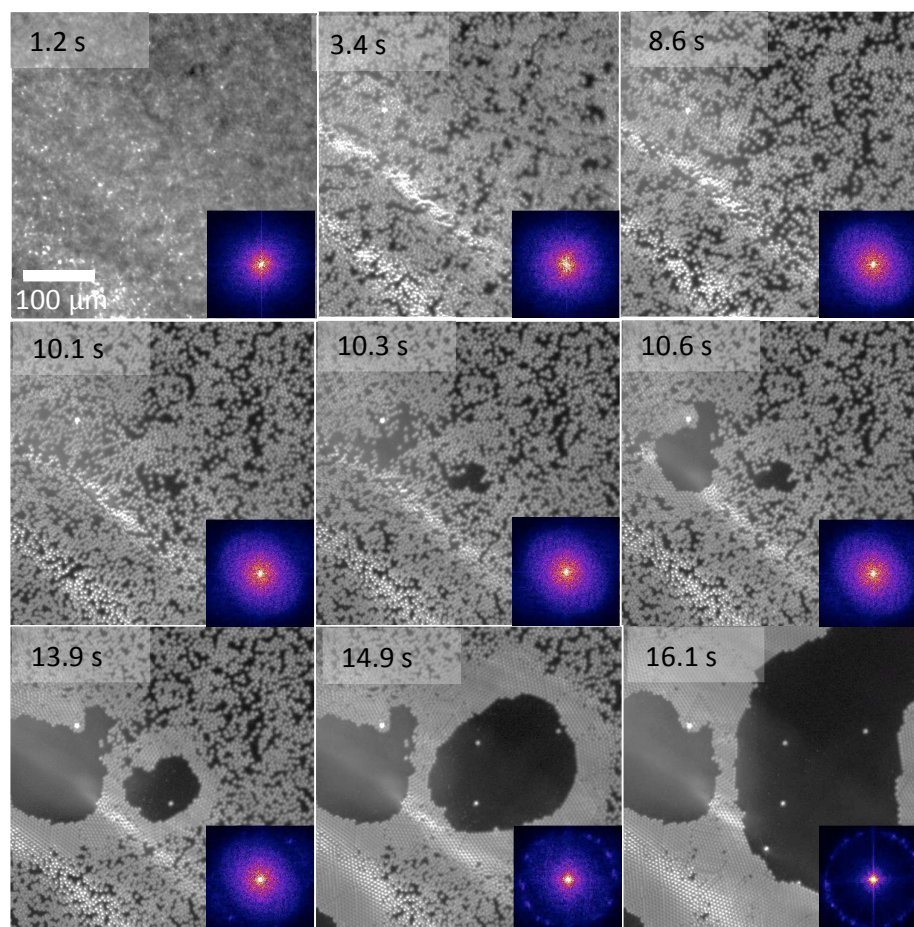


Figure 1. Series of stroboscopic microscopy images (with corresponding FFTs) for a 25 wt% colloidal dispersion in water spun-cast at 1250 rpm.

Fig. 2 and supporting information - MOVIE #2, show the structural development of slightly increased 35 wt% colloidal dispersion, which initially behaves in a similar manner to the 25 wt% dispersion, with directional flow directed towards the bottom right of the image due to shear forces.^a However at ~ 8 s, the FFT image reveals the onset of weak 6-fold symmetry, consistent with regular close packing that is also highly visible in the real space images. The onset of this symmetry coincides with the shift from shear to evaporative thinning. During this evaporative thinning only the

^a The direction of flow is different between the 25 and 35 wt% samples and is related to the synchronisation between the motor and the illumination source, which has three possible positions and therefore three different orientations about the center of rotation.

dispersant is being removed from the system, with the particle concentration increasing. Ordering occurs in order to maximise the packing of the particles resulting in the formation of a more ordered morphology (8 – 20 s), the evolution of which is highly apparent in both the real space and reciprocal space images. The FFTs show that despite the high degree of crystallinity, the structure is polycrystalline. After 20 s, the film thins further and the appearance of holes in the wetting film, results in capillary induced ordering, occurring due to incomplete particle coverage.

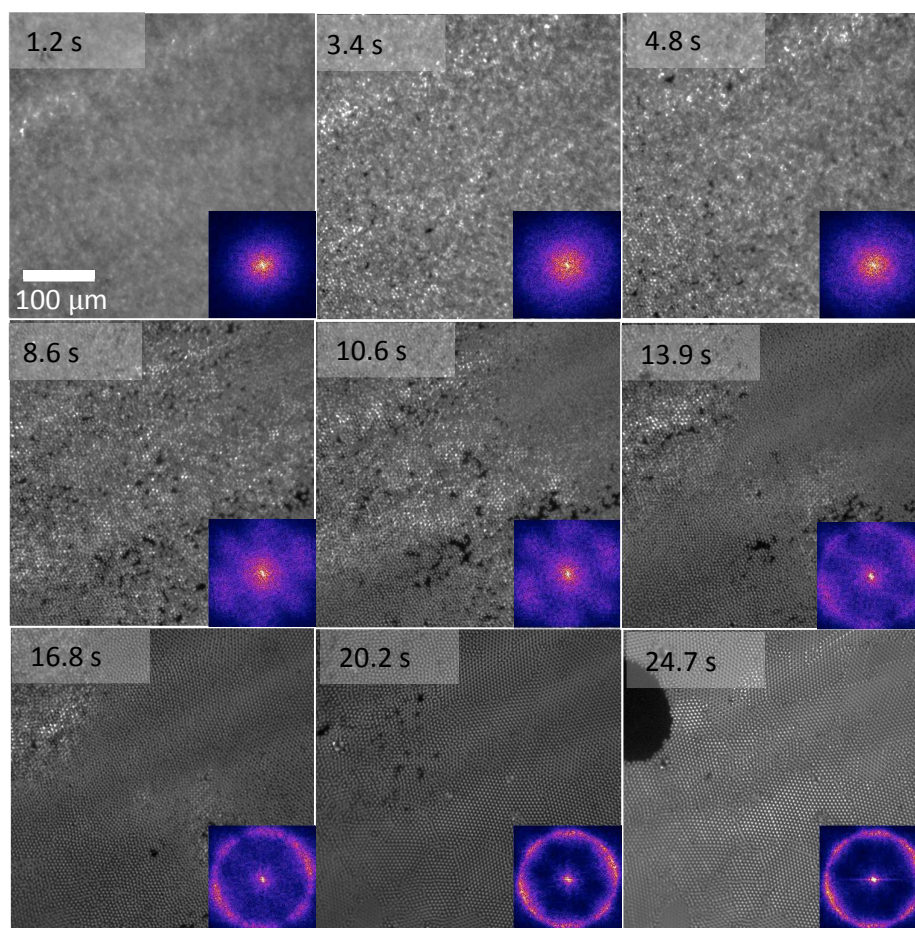


Figure 2. Series of stroboscopic microscopy images (with corresponding FFTs) for a 35 wt% colloidal dispersion in water spun-cast at 1250 rpm.

Increasing the colloid content further to 45 wt% (**Fig 3. Supporting information - MOVIE #3**) results in the dispersion exhibiting regular close packed structures even earlier, at ~ 2 s, which are highly apparent in both the real and reciprocal space images (occurring significantly earlier than the in 35 wt% dispersion), during the shear thinning stage, which stops at approximately 8 s as evaporative thinning begins to dominate. During this thinning stage a large degree of re-organisation of the colloids occurs. The 45 wt% dispersion forms ordered structures earlier on in the thinning process due to the high initial concentration of colloid particles, making regular close packing favourable so as to arrange the greater number of colloid particles. The morphology becomes fixed at ~ 15 s and after this we observe a drying front sweeping across the film as the remains of the dispersant evaporates. In this case there is an excess of particles for complete surface coverage and so a multilayer is formed (as opposed to the monolayers and incomplete monolayers formed by the 35 and 25 wt% dispersions, respectively). Additionally, the drying fronts are moving over packed layers and are unable drag the structure in more ordered array as seen with the lower weight percentage mixtures. The final structure formed is a highly crystalline, multilayer colloidal crystal containing both face centred and body centred packed regions, confirmed by the range of lengthscale in the FFT image, with small crystalline regions separated by defects. Such behaviour often occurs in films formed through horizontal deposition methods, where defects (e.g. vacancies or particles of the wrong size) result in lateral variations in the lateral packing.²

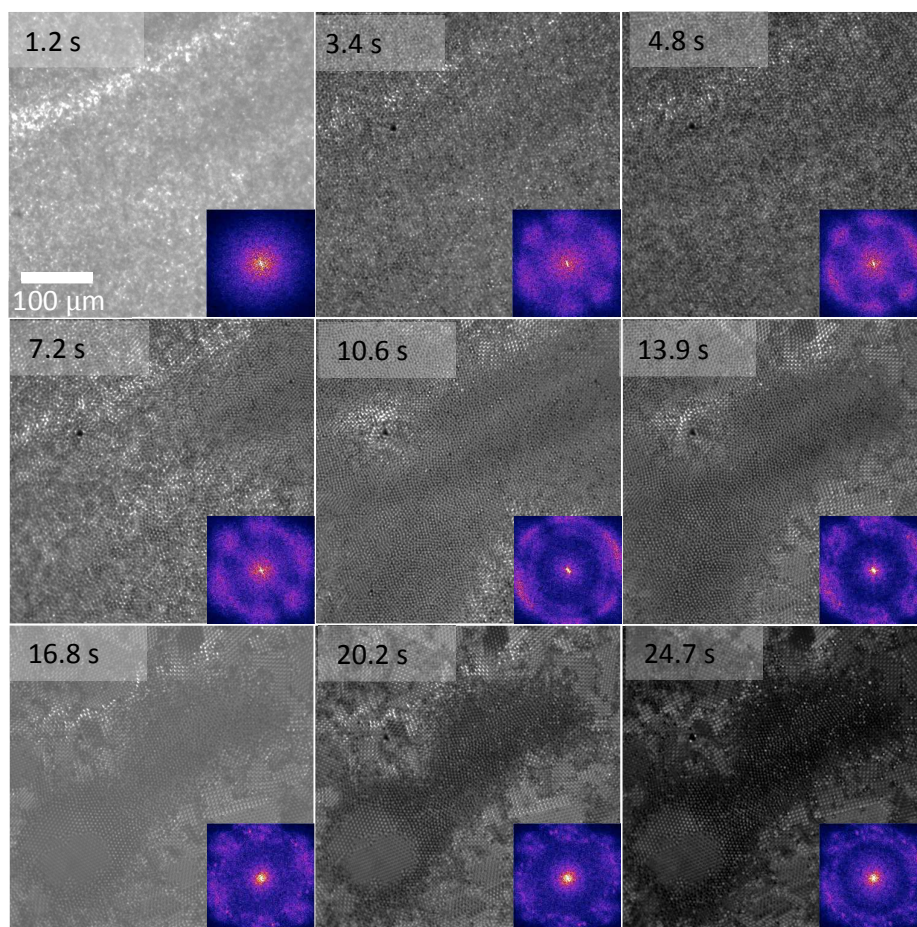


Figure 3. Series of stroboscopic microscopy images (with corresponding FFTs) for a 45 wt% colloidal dispersion in water spun-cast at 1250 rpm.

The behaviour observed for these colloidal dispersion spun-cast from water at varying concentrations show two distinct ordering mechanisms, where ordering may occur due to capillary drying fronts or simply due to packing constraints arising due to high particle concentration, reducing the inter-particle separation.

In order to investigate the role of the dispersant volatility, colloidal dispersions were made up in ethanol (vapour pressure = 5.83 kPa, compared to that of water = 2.30 kPa at 20 °C) at similar particle concentrations of 25, 35 and 45 wt%. *In situ* stroboscopic microscopy data for the comparable 25 wt% colloidal dispersion in ethanol, spun-cast at 1250 rpm is shown in Figure 4. Unlike the dispersions spun-

cast from water there is no apparent radial flow, indicating that even early on in the spin-coating process thinning is already dominated by evaporation of the dispersant. At 1.5 s a densely packed monolayer forms. The FFT image shows the presence of six faint, large symmetric spots, indicating the presence of regular close packed regions within the evolving structure. The strength of this symmetry increased between $\sim 2 - 10$ s (the spots become smaller, and more intense), indicating that the structure undergoes a degree of re-organisation, forming more uniform crystalline domains. However, after 10 s the strength of this symmetry appears to become significantly weaker. Due to the formation of a number of random close packed layers on top of this initial monolayer. We attribute this to a highly disordered two dimensional structure, which forms in this system due to the rapid evaporation of the dispersant preventing particles being incorporated into equilibrium positions in the particle arrays, and instead the particles become trapped in non-equilibrium, disordered arrangements. In effect, a skin of random packed particles is formed.

Similarly to the 25 wt% dispersion in ethanol, when 35 and 45 wt% dispersions, where spun-cast the particles formed highly disordered arrangements and did not show the same morphological evolution observed for the dispersions spun-cast from water. As such, results for the 35 and 45 wt% dispersions in ethanol are available in the supporting information (**SI Fig. 1 and 2**). Early on in the spin-coating ($t < 4$ s), a large number of particles appear out of focus for dispersions spun-cast from either water or ethanol at various concentrations. As the focal plane lies on the substrate, we can infer that any out of focus particles are therefore above the substrate. For the dispersions spun-cast from ethanol, a larger proportion of particles are found to be above the substrate and surface monolayer region. We

attribute this behaviour to the occurrence of Marangoni flows, that act to drag the particles towards the evaporating surface of the thinning film. SEM micrographs of the final structures of micrographs of the final structures of colloidal dispersions spun cast from water and ethanol at concentrations of 25 wt% and 45 wt% are shown in **SI Fig. 3**.

The formation of a skin layer of particles was modelled by Routh and Zimmerman.²⁷ The concept of their work was that in a system where diffusion dominates the particles remain uniformly distributed. However, if the diffusive processes are weak, evaporation of the dispersant results in a non-uniform particle distribution with the formation of a skin.²⁸ Reyes and Duda performed Monte Carlo simulations showing that at slow evaporation rates particles are able to crystallise, whilst for faster evaporation rates random close packed structures will form.²⁹ It is possible that for the solutions spun-cast from ethanol, rapid evaporation, results in a colloidal glass transition,^{30,31} where the particles are jammed and unable to rearrange into thermodynamically favourable arrangements.³²

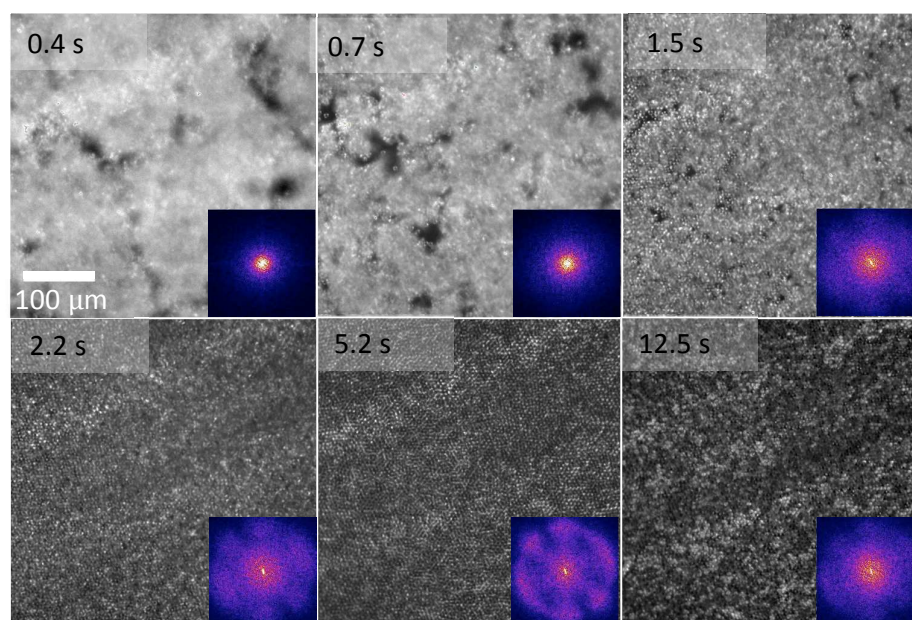


Figure 4. Series of stroboscopic microscopy images (with corresponding FFTs) for a 25 wt% colloidal dispersion in ethanol spun-cast at 1250 rpm.^b

Through studying the assembly processes of polystyrene colloids from both water and ethanol we have been able to show how the dispersant volatility has a large impact upon the uniformity and order of the final morphology with the density of particle coverage and the rate of evaporation determining whether ordering may occur and whether it takes place via the formation of capillary fronts or through the re-organisation of particles.

In order to further explore these relationships we have studied colloidal dispersions in mixtures of water and ethanol. Figures 5 – 7 show the ordering of spin-coated 25 wt% colloidal dispersions made up in water:ethanol mixtures mass compositions of 6:4, 1:1 and 4:6, having combined vapour pressures of 3.8, 4.2, 4.5 kPa, respectively.

^b Only six frames are presented in Fig. 4 and Supporting Fig. 1 and 2 as there is significantly less evolution in structure between the frames.

Data for the 6:4 (water:ethanol, 25 wt%) dispersion is shown in **Fig 5. Supporting information - MOVIE #5**. Early on during the coating process (~ 1.25 s) the dispersion behaves in a similar manner to that of the pure ethanol dispersion, forming a monolayer (with weak six-fold symmetry), containing a large number of voids, with a large amount of particle flow occurring above the image plane. As the film thins voids become filled by particles which sediment. By 3 s the monolayer contains no voids and begins to flow (from the bottom to the top of the image plane) due to shear forces. This shear flow induces further ordering within the particles, which can be readily seen in the FFT images. At ~ 10 s a number of particles become pinned at the substrate surface and much slower particle flow may be observed until ~ 34 s, after which, ordering proceeds via capillary effects occurring due to the presence of voids in the morphology.

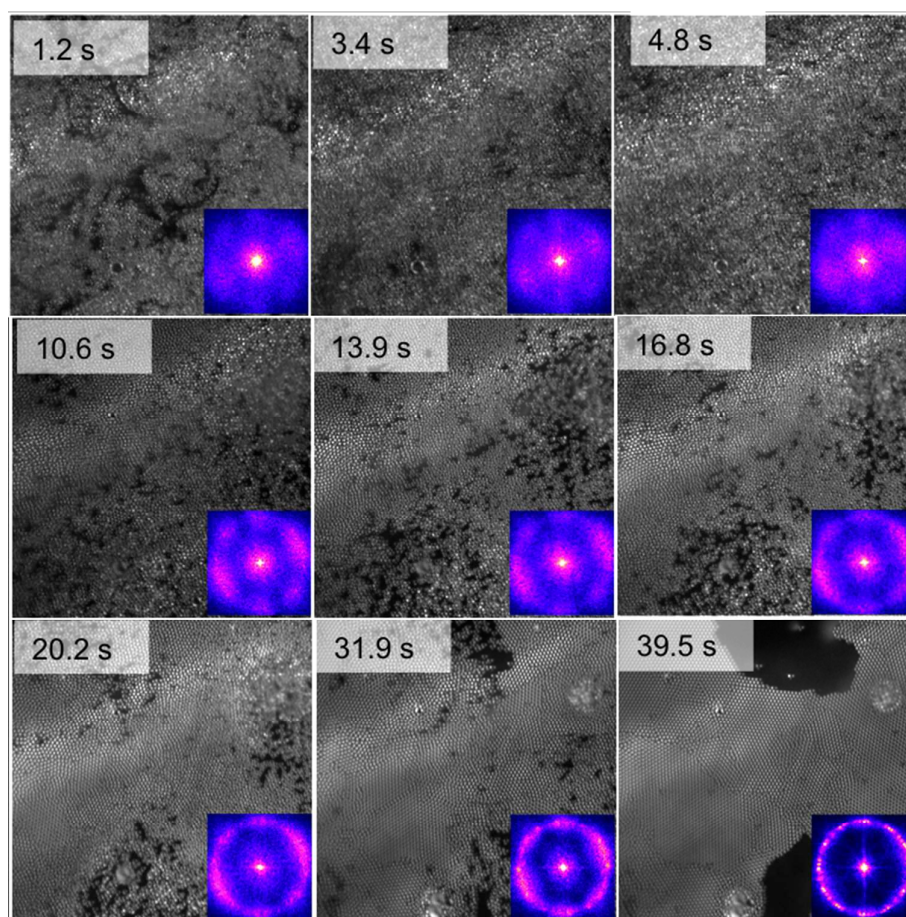


Figure 5. Series of stroboscopic microscopy images (with corresponding FFTs) for a 25 wt% colloidal dispersion in a water:ethanol mixture (6:4) spun-cast at 1250 rpm.

The colloidal dispersion spun-cast from a 1:1 mixture of water and ethanol (Fig. 6 Supporting information - MOVIE #6) initially forms a monolayer on the substrate surface (~ 1 s). The coverage of which, increases through the sedimentation of subsequent particles as a result of particle flow. The FFT images reveal that the monolayer shows weak six-fold symmetry from 2.4 s onwards and by ~ 3.5 s the monolayer appears to completely cover the substrate. Particle flow occurs above the monolayer, until 8.9 s, after which the monolayer begins to order due to the shear forces. Initially, this process involves the flow of particles to fill any void

spaces. At ~ 24 s the whole monolayer begins to flow (towards top right of image) as a consequence of shear. During this period the FFT images reveal a dramatic increase in the crystallinity of the colloid array structure and at ~ 29 s, it is possible to observe clear rotation of crystallisation spots evoked by shear induced re-organisation and we attribute this to be an example of shear induced crystallisation.

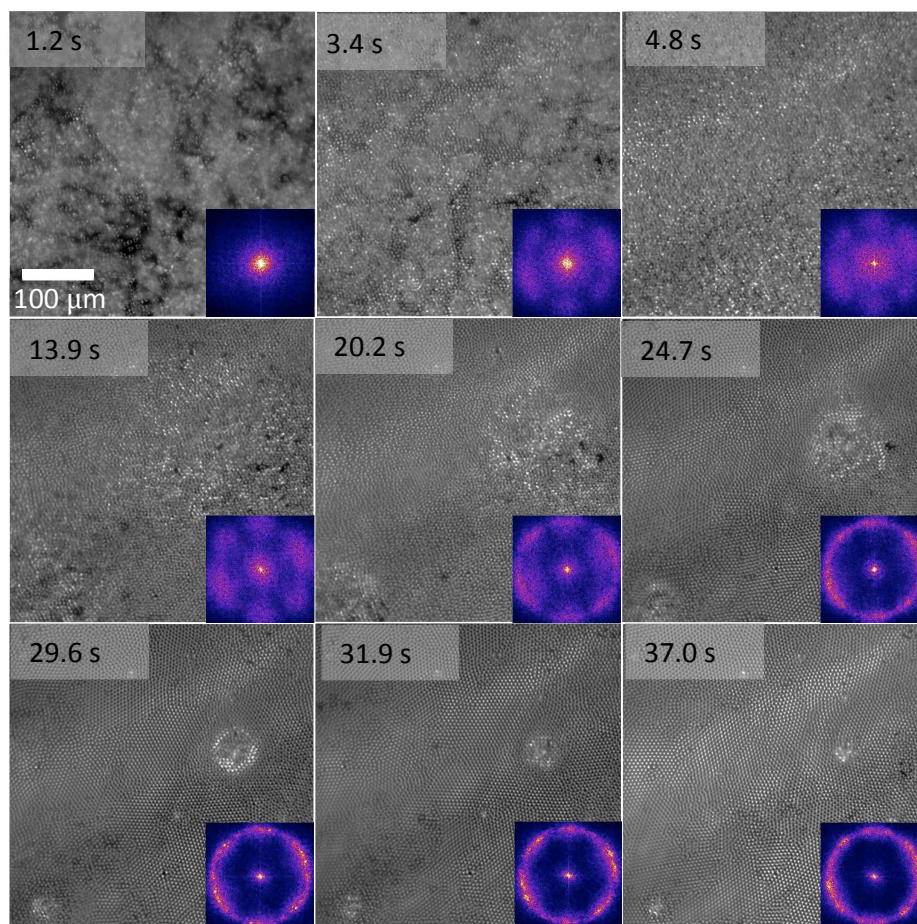


Figure 6. Series of stroboscopic microscopy images (with corresponding FFTs) for a 25 wt% colloidal dispersion in a water:ethanol mixture (1:1) spun-cast at 1250 rpm.

Data for the 4:6 dispersion (**Fig 7. Supporting information - MOVIE #7**) shows that an initial ordered monolayer forms early on (~ 1 s), which then re-orders due to shear forces (1 – 5 s) resulting in the formation of a highly ordered regular close packed structure. This structure forms in a similar manner to that of the 1:1

dispersion, however, in the case of the 4:6 dispersion this ordering is disrupted due to excessive shear, resulting in the formation of voids and subsequent capillary ordering. This capillary induced ordering occurs between 20 and 25 s (as described earlier), resulting in the formation of a highly ordered regular close packed polycrystalline structure, containing large voids.

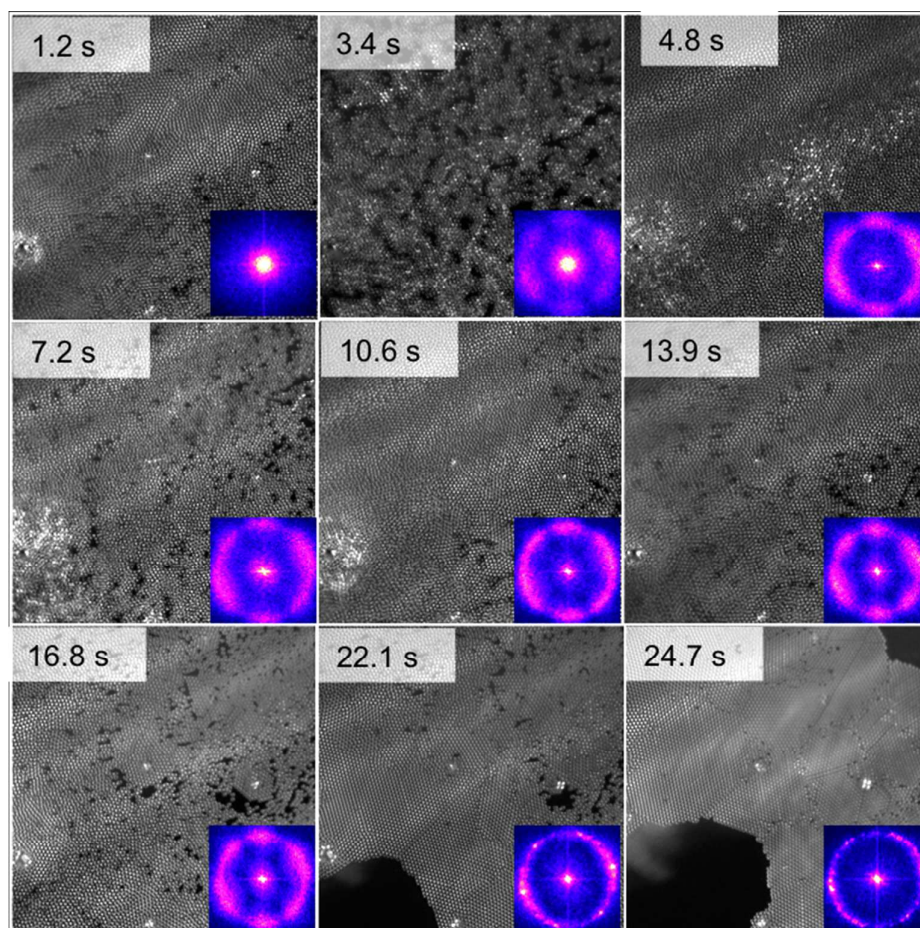


Figure 7. Series of stroboscopic microscopy images (with corresponding FFTs) for a 25 wt% colloidal dispersion in a water:ethanol mixture (4:6) spun-cast at 1250 rpm.

For the water:ethanol colloidal dispersions it is evident that early on colloids are distributed at both the substrate and above the image plane (towards the film-air interface) due to both particle sedimentation and evaporation inducing the formation of a skin.^{27,33} As the film thins the particles become constrained and only a

single monolayer at the substrate is observed. For the water:ethanol dispersion with the lowest volume fraction of ethanol, capillary effects dominate the ordering of the final structure, whilst for the 1:1 water:ethanol dispersion shear induced re-ordering leads to the formation of highly ordered structures and for the dispersion with the highest volume fraction of ethanol, excessive shear leads to the formation of holes within the system and so hole formation induces a large degree of order. This excessive shear is analogous to shear-induced melting described by Ackerson *et al.*³⁴

In Fig. 8 the different mechanisms of colloidal ordering are summarised. We have directly observed ordering occurring due to high concentrations of colloid particles (where volatility is relatively low), resulting in the formation of ordered HCP and FCP arrays. Conversely when the system is spun-cast from a much more volatile solvent, highly disordered non-equilibrium arrangements of particles form. When spin-coating a low concentration, low volatility dispersion, ordering is dominated by the occurrence of capillary drying fronts that form from the formation of holes within the wetting film. At a certain volatility, of an intermediate value between that of water and ethanol, ordering occurs predominantly via shear forces. Finally when the volatility is further increased above this intermediate value at the shear ordering regime, excessive shear leads to the formation of holes within the system and so hole formation induces a large degree of order. In this study, we have gained new insights into the mechanisms of colloidal ordering during spin-coating through studying the development of lateral structure. In order to fully understand the process it is imperative that further information on the distribution of particles perpendicular to the substrate is obtained, in order to understand the role sedimentation, evaporation and Marangoni flows play.

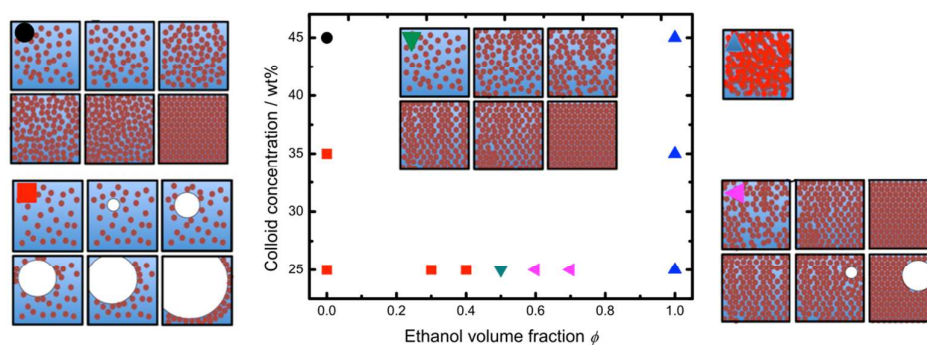


Figure 8. Schematic summarising the observed mechanisms of colloidal ordering that depend upon the colloid concentration and the solvent volatility, where the mechanisms ordering are; ●, concentration induced ■, capillary induced ▼, shear induced □, shear collapse followed by capillary induced and ▲, disordered structures.

Methodology

The stroboscopic microscope set-up is described in detail in references 19 to 22. A small DC motor acts as a spin-coater, which is mounted directly under a 40X objective (Nikon CFI S Plan Fluor ELWD 40X). The current supply to the motor shows sharp dips as the brushes pass between commutators and this is used to trigger a 50 μ s pulse of white light from three LEDs (Cree X-Lamp, XP-G2, cool white). The pulse is also used to trigger image collection, occurring once per revolution. The coupling of the triggering of illumination and image capture to rotation means that collected images appear static, irrespective of spin-speed. An Andor iXON (897+) was used, which has a field of view of 464 \times 464 μ m when used in conjunction with an ELWD \times 40 objective, respectively.

Micrometer-sized PS particles, with a number-average diameter of 5.16 μ m and a polydispersity of 1.01 (determined by SEM) were purchased from Microbeads,

Norway. The micrometer-sized polymer particles are stabilised with anionic sodium dodecyl sulfate surfactant in combination with a cellulosic stabiliser.

Circular glass microscope cover slips were utilised as the substrate and where used as supplied. Each substrate was placed on a transparent perspex chuck (15mm \varnothing , 10mm thick). 50 μ l of the colloidal dispersion was dispensed onto the substrate and then spun at 1250 rpm, with data collected for 1000 exposures, corresponding to 48 s.

Acknowledgments

This work was partially supported by JSPS Postdoctoral Fellowship for Overseas Researchers (PE13510) from Japan Society for the Promotion of Science.

References

- 1 Keddie, J. L. Film formation of latex. *Materials Science and Engineering: R: Reports* **21**, 101-170, doi:[http://dx.doi.org/10.1016/S0927-796X\(97\)00011-9](http://dx.doi.org/10.1016/S0927-796X(97)00011-9) (1997).
- 2 Keddie, J. L. & Routh, A. F. *Fundamentals of latex film formation: processes and properties*. (Springer, 2010).
- 3 Winnik, M. A. Latex film formation. *Current Opinion in Colloid & Interface Science* **2**, 192-199, doi:[http://dx.doi.org/10.1016/S1359-0294\(97\)80026-X](http://dx.doi.org/10.1016/S1359-0294(97)80026-X) (1997).
- 4 Deegan, R. D. *et al.* Capillary flow as the cause of ring stains from dried liquid drops. *Nature* **389**, 827-829, doi:Doi 10.1038/39827 (1997).
- 5 Wijnhoven, J. E. G. J. & Vos, W. L. Preparation of Photonic Crystals Made of Air Spheres in Titania. *Science* **281**, 802-804, doi:10.1126/science.281.5378.802 (1998).
- 6 Pusey, P. N. & Vanmegen, W. Phase-Behavior of Concentrated Suspensions of Nearly Hard Colloidal Spheres. *Nature* **320**, 340-342, doi:Doi 10.1038/320340a0 (1986).
- 7 Jones, R. A. L. *Soft condensed matter*. (Oxford University Press, 2002).
- 8 Denkov, N. *et al.* Two-dimensional crystallization. (1993).
- 9 Kralchevsky, P. A. & Denkov, N. D. Capillary forces and structuring in layers of colloid particles. *Current Opinion in Colloid & Interface Science* **6**, 383-401, doi:[http://dx.doi.org/10.1016/S1359-0294\(01\)00105-4](http://dx.doi.org/10.1016/S1359-0294(01)00105-4) (2001).
- 10 Ohara, P. C. & Gelbart, W. M. Interplay between hole instability and nanoparticle array formation in ultrathin liquid films. *Langmuir* **14**, 3418-3424, doi:Doi 10.1021/La971147f (1998).

- 11 Jiang, P. & McFarland, M. J. Large-Scale Fabrication of Wafer-Size Colloidal Crystals, Macroporous Polymers and Nanocomposites by Spin-Coating. *Journal of the American Chemical Society* **126**, 13778-13786, doi:10.1021/ja0470923 (2004).
- 12 Mihi, A., Ocana, M. & Miguez, H. Oriented colloidal-crystal thin films by spin-coating microspheres dispersed in volatile media. *Adv. Mater. (Weinheim, Ger.)* **18**, 2244-2249, doi:10.1002/adma.200600555 (2006).
- 13 Chen, J. *et al.* Controllable fabrication of 2D colloidal-crystal films with polystyrene nanospheres of various diameters by spin-coating. *Applied Surface Science* **270**, 6-15, doi:<http://dx.doi.org/10.1016/j.apsusc.2012.11.165> (2013).
- 14 Bartlett, A. P., Pichumani, M., Giuliani, M., González-Vinas, W. & Yethiraj, A. Modified Spin-coating Technique to Achieve Directional Colloidal Crystallization. *Langmuir* **28**, 3067-3070, doi:10.1021/la204123s (2012).
- 15 Colson, P., Cloots, R. & Henrist, C. Experimental Design Applied to Spin Coating of 2D Colloidal Crystal Masks: A Relevant Method? *Langmuir* **27**, 12800-12806, doi:10.1021/la202284a (2011).
- 16 Mihi, A., Ocaña, M. & Míguez, H. Oriented Colloidal-Crystal Thin Films by Spin-Coating Microspheres Dispersed in Volatile Media. *Advanced Materials* **18**, 2244-2249, doi:10.1002/adma.200600555 (2006).
- 17 Arcos, C. *et al.* Orientationally correlated colloidal polycrystals without long-range positional order. *Physical Review E* **77**, 050402 (2008).
- 18 Birnie, D. Combined flow and evaporation of fluid on a spinning disk. *Phys. Fluids* **9**, 870 (1997).
- 19 Meyerhofer, D. *Characteristics of resist films produced by spinning*. Vol. 49 (AIP, 1978).
- 20 Giuliani, M., González-Vinas, W., Poduska, K. M. & Yethiraj, A. Dynamics of crystal structure formation in spin-coated colloidal films. *The Journal of Physical Chemistry Letters* **1**, 1481-1486 (2010).
- 21 Shereda, L. T., Larson, R. G. & Solomon, M. J. Local stress control of spatiotemporal ordering of colloidal crystals in complex flows. *Physical review letters* **101**, 038301 (2008).
- 22 Toolan, D. T., Pullan, N., Harvey, M. J., Topham, P. D. & Howse, J. R. In situ studies of phase separation and crystallization directed by Marangoni instabilities during spin-coating. *Adv Mater* **25**, 7033-7037, doi:10.1002/adma.201302657 (2013).
- 23 Toolan, D. T. W. *et al.* Direct observation of morphological development during the spin-coating of polystyrene-poly(methyl methacrylate) polymer blends. *Journal of Polymer Science Part B: Polymer Physics* **51**, 875-881, doi:10.1002/polb.23288 (2013).
- 24 Toolan, D. T. W., Hodgkinson, R. & Howse, J. R. Stroboscopic Microscopy-Direct Imaging of Structure Development and Phase Separation During Spin-Coating. *Journal of Polymer Science Part B-Polymer Physics* **52**, 17-25, doi:10.1002/Polb.23410 (2014).
- 25 Toolan, D. T. W., Parnell, A. J., Topham, P. D. & Howse, J. R. Directed phase separation of PFO:PS blends during spin-coating using feedback controlled in situ stroboscopic fluorescence microscopy. *Journal of*

- Materials Chemistry A* **1**, 3587-3592, doi:Doi 10.1039/C3ta01530k (2013).
- 26 Elbaum, M. & Lipson, S. G. How does a thin wetted film dry up? *Physical Review Letters* **72**, 3562-3565 (1994).
- 27 Routh, A. F. & Zimmerman, W. B. Distribution of particles during solvent evaporation from films. *Chemical engineering science* **59**, 2961-2968 (2004).
- 28 Routh, A. F. Drying of thin colloidal films. *Reports on Progress in Physics* **76**, 046603 (2013).
- 29 Reyes, Y. & Duda, Y. Modeling of Drying in Films of Colloidal Particles. *Langmuir* **21**, 7057-7060, doi:10.1021/la050167b (2005).
- 30 Pusey, P. N. & van Megen, W. Observation of a glass transition in suspensions of spherical colloidal particles. *Physical Review Letters* **59**, 2083-2086 (1987).
- 31 Mason, T. G. & Weitz, D. A. Linear Viscoelasticity of Colloidal Hard Sphere Suspensions near the Glass Transition. *Physical Review Letters* **75**, 2770-2773 (1995).
- 32 Narita, T., Hébraud, P. & Lequeux, F. Effects of the rate of evaporation and film thickness on nonuniform drying of film-forming concentrated colloidal suspensions. *The European Physical Journal E* **17**, 69-76, doi:10.1140/epje/i2004-10109-x (2005).
- 33 Cardinal, C. M., Jung, Y. D., Ahn, K. H. & Francis, L. F. Drying regime maps for particulate coatings. *Aiche J.* **56**, 2769-2780, doi:10.1002/aic.12190 (2010).
- 34 Ackerson, B. J. & Clark, N. A. Shear-induced melting. *Phys. Rev. Lett.* **46**, 123-126, doi:10.1103/PhysRevLett.46.123 (1981).

